Journal of Cell Science 111, 2085-2095 (1998)
Printed in Great Britain © The Company of Biologists Limited 1998
JCS7249



# Cytoplasmic dynamics of myosin IIA and IIB: spatial 'sorting' of isoforms in locomoting cells

**John Kolega**

Department of Anatomy and Cell Biology, State University of New York at Buffalo School of Medicine and Biomedical Sciences, 3435 Main Street, Buffalo, New York, USA
(e-mail: kolega@buffalo.edu)

*Accepted 20 May; published on WWW 15 July 1998*

## SUMMARY

**Different isoforms of non-muscle myosin II have different distributions in vivo, even within individual cells. In order to understand how these different distributions arise, the distribution and dynamics of non-muscle myosins IIA and myosin IIB were examined in cultured cells using immunofluorescence staining and time-lapse imaging of fluorescent analogs. Cultured bovine aortic endothelia contained both myosins IIA and IIB. Both isoforms distributed along stress fibers, in linear or punctate aggregates within lamellipodia, and diffusely around the nucleus. However, the A isoform was preferentially located toward the leading edge of migrating cells when compared with myosin IIB by double immunofluorescence staining. Conversely, the B isoform was enriched in structures at the cells' trailing edges. When fluorescent analogs of the two isoforms were co-injected into living cells, the injected myosins distributed with the same disparate localizations as endogenous myosins IIA and IIB. This indicated that the ability of the myosins to 'sort' within the cytoplasm is intrinsic to the proteins themselves, and not a result of localized synthesis or degradation. Furthermore, time-lapse imaging of injected analogs in living cells revealed differences in the rates at which the two isoforms rearranged during cell movement. The A isoform appeared in newly formed structures more rapidly than the B isoform, and was also lost more rapidly when structures disassembled. These observations suggest that the different localizations of myosins IIA and IIB reflect different rates at which the isoforms transit through assembly, movement and disassembly within the cell. The relative proportions of different myosin II isoforms within a particular cell type may determine the lifetimes of various myosin II-based structures in that cell.**

Key words: Cell motility, Cytoskeleton, Myosin heavy chain, Endothelium, Fluorescent analog

## INTRODUCTION

Myosin II, the mechanoenzyme responsible for muscle contraction (Huxley, 1969), is also present in most non-muscle cells. In non-muscle cells, myosin II is involved in cytoplasmic contractility (Condeelis and Taylor, 1977), cytokinesis (DeLozanne and Spudich, 1987; Knecht and Loomis, 1987), capping of cell-surface components (Pasternak et al., 1989), and polarization of cell locomotion (Wessels and Soll, 1990; Wessels et al., 1988). These diverse functions require considerable movement of myosin II within the cell, and non-muscle myosin II is much more plastic in the cytoplasm than is skeletal-muscle myosin. Non-muscle myosin II forms smaller, less long-lived filaments in vivo, and the assembly of these filaments in physiological salt concentrations can be regulated by phosphorylation of myosin II's regulatory light chains (Tan et al., 1992; Trybus, 1991). In this regard, non-muscle myosin II is very similar to smooth-muscle myosin II (Sellers, 1991; Trybus, 1991).

Because of the similarity in regulation of smooth- and non-muscle myosin II, fluorescent analogs of smooth-muscle myosin II have often been used to examine the behavior of myosin II in non-muscle cells (Giuliano and Taylor, 1990; Kolega et al., 1991; McKenna et al., 1989; Sanger et al., 1989). When smooth-muscle analogs of myosin II are injected into non-muscle cells, their distribution parallels the distribution of endogenous myosin II remarkably well. This raises the question of why different isozymes exist in smooth- and non-muscle cells, if they can perform the same functions in the cytoplasm. Non-muscle myosin II itself consists of multiple isozymes with at least two different genes producing heavy chains of non-muscle myosin II (Katsuragawa et al., 1989). The different heavy-chain gene products, designated MHC-A and MHC-B, can be distinguished by antibodies to unique sequences near the carboxy termini of the two peptides (Maupin et al., 1994; Murakami et al., 1991). Immunolocalization of MHC-A and MHC-B in cultured cells indicates that the two isoforms have different sub-cellular distributions. This is most dramatic in neurons, where myosin IIB (i.e. myosin II containing the MHC-B heavy chain) is considerably elevated over myosin IIA in the margins of the growth cone (Cheng et al., 1992; Rochlin et al., 1995). Myosin

IIB is also distributed differently from myosin IIA in a variety of other non-muscle cells in culture. For example, in Xenopus A6 and XTC cells, myosin IIB is found in peripheral fibers where myosin IIA is absent (Kelley et al., 1996). In contrast, in human melanoma cells (Maupin et al., 1994) and non-neuronal cells from rat ganglia (Rochlin et al., 1995), it is myosin IIA that is highly enriched over myosin IIB in peripheral fibers. Myosins IIA and IIB also differ in the extent to which they are localized in the cleavage furrow during cytokinesis (Maupin et al., 1994; Conrad et al., 1995; Kelley et al., 1996). Although a consistent pattern to these differences has not yet appeared, they suggest that myosins IIA and IIB may perform different functions, or at least contribute differently to those functions in different parts of the cell.

In order to learn how these contributions might differ, it is helpful to understand how different isoforms attain their distinct distributions. Myosin II is very dynamic in non-muscle cells, with myosin II-containing structures continuously assembling, moving and disassembling (Giuliano and Taylor, 1990; McKenna et al., 1989; Sanger et al., 1989). How are specific isoforms of myosin II preferentially kept within or excluded from various regions of the cell during these rearrangements? Do they possess intrinsic properties that determine their distinct intracellular distributions? Kelly et al. (1996) recently showed that myosins IIA and IIB move actin filaments at different rates in vitro, which could reflect different movements of the isoforms in situ. Alternatively, myosins IIA and IIB may be synthesized at different sites, as has been observed for actin isoforms (Hoock et al., 1991). Wiseman et al. (1997) recently demonstrated that the mRNA for skeletal-muscle myosin heavy chains contains a sequence that can direct the sub-cellular localization of message in the cytoplasm of cultured myotubes. Different isoform distributions could also be due to different rates of turnover. Yet another possibility is that myosins IIA and IIB do not really distribute differently at all: the small epitopes that distinguish the two isoforms could easily be masked, particularly in the tightly packed filaments that myosin II can form. If, for example, local binding of cytoskeletal proteins were to cover one of the epitopes, it would appear by immunolocalization as if that isoform were absent, even if both isoforms were equally represented throughout the cell.

In the present study, different isoforms of myosin II were fluorescently labeled and injected into cultured endothelial cells in order to observe the dynamics of their behavior in vivo. This demonstrated that isoforms can sort themselves to specific locations in the cytoplasm. Injected non-muscle myosins IIA and IIB adopted different distributions that parallel the distributions of endogenous myosins IIA and IIB. Interestingly, fluorescently labeled smooth-muscle myosin II co-distributed with non-muscle myosin IIA. In addition, differences in the movements of the various isoforms during cell migration were observed. The results indicate that different myosin II isoforms possess inherent characteristics that influence the rate of their intracellular rearrangements, and this effects their sub-cellular localization when cells are moving and changing shape.

## MATERIALS AND METHODS

### Cells

Bovine aortic endothelial cells were cultured from an early passage primary culture obtained from the laboratory of Dr Scott Diamond (University of Pennsylvania), and were confirmed as endothelial cells by staining for Factor VIII and by specific binding and uptake of low-density lipoproteins. They were cultured in Dulbecco's modified Eagle's medium plus 10% fetal bovine serum with 10 mM Hepes, pH 7.4, and were used between the 12th and 18th passage after their original isolation. COS fibroblasts from African green monkey kidneys were from American Type Culture Collection (Rockville, MD) and were cultured in the same medium.

### Immunofluorescence and immunoblotting

Cells were fixed and permeabilized as described by Conrad et al. (1993), except that 3.7% formaldehyde was used instead of 2%. For indirect immunofluorescence, specimens were stained with antibodies that were raised against synthetic peptides corresponding to the unique carboxy termini of MHC-A (myosin II heavy chain, isoform A), and MHC-B (myosin II heavy chain, isoform B) (Maupin et al., 1994; Phillips et al., 1995). These antibodies were generously provided by R. Adelstein (National Institutes of Health), and do not recognize other myosin II heavy chains. For direct immunofluorescence, these antibodies were labeled with rhodamine or cy5 as follows: A 10-fold molar excess of reactive dye (tetramethylrhodamine-isothiocyanate from Sigma Chemical Corporation, St Louis, MO, or cy5-monofunctional NHS-ester from Amersham Life Sciences, Arlington Heights, IL) was added to a 1 mg/ml solution of antibody (IgG) in 0.1 M sodium bicarbonate, pH 8.3. The mixture was incubated for 1 hour at 20°C, the reaction stopped by the addition of hydroxylamine to 0.15 M, and any unbound dye removed by chromatography over G-25 Sephadex.

The same antibodies against MHC-A and MHC-B were used for western blotting, along with a polyclonal antibody against smooth- and non-muscle myosin II (Biomedical Technologies, Inc., Stoughton, MA). The secondary antibody for western blotting was an affinity-purified, peroxidase-conjugated goat antibody against rabbit IgG heavy and light chains (Kirkegaard and Perry Laboratories, Gaithersburg, MD), which was visualized using diaminobenzidine as a substrate. The intensity of staining on western blots was quantified by image densitometry, as previously described (Kolega, 1997).

### Fluorescently labeled myosin II

Smooth-muscle myosin II was isolated from frozen turkey gizzards (Pel-Freeze Biologicals, Rogers, AK) using the procedures described by DeBiasio et al. (1988) for chicken-gizzard myosin II. Myosin IIA was isolated from bovine platelets by the method of Daniel and Sellers (1992), and brain myosin II was isolated from bovine brains using essentially the procedure of Li et al. (1994), except that Mops was used in place of imidazole as the buffering agent in all solutions, and a 40-60% rather than 35-65% ammonium sulfate cut was taken. These myosins were fluorescently labeled with rhodamine or cy5 as previously described (DeBiasio et al., 1988; Kolega, 1997, 1998). The labeled myosins each retained activity that was comparable to unlabeled myosin II in all of the following: (1) reversible assembly into thick filaments, (2) actin-activatable MgATPase, (3) phosphorylation by myosin light chain kinase, (4) increased MgATPase upon light-chain phosphorylation, and (5) interconversion between 6S and 10S conformations. The biochemical characterization of these analogs is described elsewhere (DeBiasio et al., 1988; Hahn et al., 1993; Kolega, 1997, 1998).

### Microwounds

To examine the early stages of lamellipodial protrusion, BAECs were allowed to grow until they formed a confluent monolayer. 3 days after reaching confluence, cells within the monolayer were microinjected with fluorescent analogs, and the analogs were allowed to equilibrate in the cell for at least 3 hours. Fluorescent cells were then located and the formation of new lamellipodia was induced by scraping away an adjacent cell with a micromanipulated needle. Redistribution of the analogs was followed by acquiring fluorescence images at 30-second intervals during and after the micromanipulation.

### Image acquisition

Fluorescence microscopy was performed through a Zeiss Axiovert 135 microscope with a 100 W mercury arc lamp for excitation illumination, using a ×100 Plan-NEOFLUAR oil-immersion objective. Fluorescence images were acquired by using Oncor-Image software (Oncor, Gaithersburg, MD) to sum 32 frames of the video output from a Paultek CCD camera, equipped with a Gen II-MCP intensifier (Paultek Imaging, Grass Valley, CA). The pixel density in the final digitized images was 4.2 pixels/μm. For some time-lapse sequences, an additional ×1.6 lens was placed between the objective and the camera increasing the pixel density to 6.7 pixels/μm. Rhodamine images were acquired through a Zeiss #14 filter set, and cy5 images through a HQ cy5 filter set (Chroma Technology; Brattleboro, VT). No bleed-through of either fluorophore could be detected at the levels of illumination used in this study.

### Image processing and analysis

For each image, background fluorescence was removed by subtracting a background image acquired from an adjacent, cell-free field in the specimen. For illustrations, images were displayed with a linear look-up table with a 0 intercept, and brightness and contrast were adjusted by changing only the slope of the look-up table. In addition, some images were sharpened using a 3×3 Laplacian kernel.

For ratio images, image pairs were checked for correct registration, background fluorescence was subtracted from each image as described above, and the total intensity of the image was calculated by integrating over all pixels. The two images in the ratio pair were then normalized to the same total intensity by multiplying the dimmer image by the quotient of the integrated intensities, and the ratio image was obtained by dividing the normalized images. Ratio images are illustrated with a linear, 0-intercept look-up table.

For the purpose of measuring regional differences in fluorescence or ratio values, images of individual cells were frequently divided into three regions: the leading, middle and trailing zones. The leading zone was defined by a line drawn perpendicular to the direction of cell migration at a point halfway between the most forward projection of the cell and the front edge of the nucleus. Everything forward of this line was taken as the 'leading zone'. Similarly, the trailing zone was defined by a line drawn halfway between the most rearward point in the cell and the rear edge of the nucleus, with the 'trailing zone' consisting of all parts of the cell behind this line. The middle zone consisted of the remainder of the cell; i.e. all the cytoplasm between the two lines defining the leading and trailing zones.

When comparing images in a time-lapse series, each image was normalized to the same total intensity: After subtracting background fluorescence, the total fluorescence intensity was integrated over the cell of interest in each image in the series. Dividing this integrated intensity into the integrated intensity for the brightest image in the series gave a correction factor for each image. Each image was then multiplied by its correction factor to produce a series in which all images had the same total intensity. This permits direct comparison between different fluorescent analogs, and also corrects for any photobleaching that occurs when multiple images are acquired.

## RESULTS

### Distribution of endogenous myosins IIA and IIB in cultured endothelial cells

Western blotting of whole-cell extracts from cultured BAECs showed that these endothelial cells contain both A and B isoforms of the non-muscle myosin II heavy chain (Fig. 1A). Using densitometry to compare the staining of heavy-chain bands in BAEC extracts with known amounts of platelet myosin II and brain myosin II, the majority (70-90%) of the myosin II in BAECs was found to be the A isoform, and the remaining 10-30% was MHC-B. Immunofluorescence staining with antibodies that are specific for the individual isoforms revealed that both isoforms are broadly distributed in the cytoplasm (Fig. 1B,C). Both MHC-A and MHC-B were highly concentrated along stress fibers, where they often displayed periodic, striated or punctate patterns. Punctate patterns were also observed in the peripheral cytoplasm. The latter pattern was similar in appearance to the myosin aggregates reported by McKenna et al. (1989) and Verkhovsky et al. (1995). A diffuse halo of staining around the nucleus was also observed.

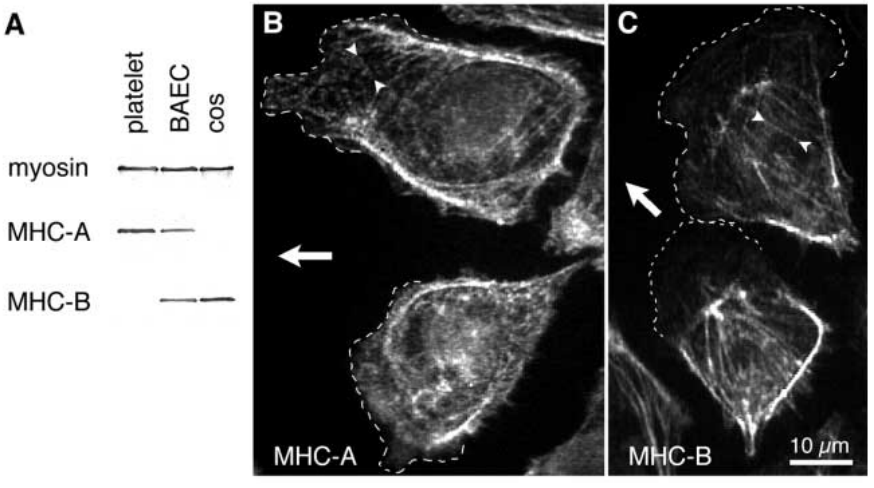


**Fig. 1.** Myosins IIA and IIB in BAECs.
(A) Western blots against myosin IIA and myosin IIB. Non-muscle myosin IIA purified from platelets, a cytoskeletal extract from BAECs, and a cytoskeletal extract from cos fibroblasts (which contain only the B heavy chain of myosin II) were run on 8.5% polyacrylamide gels and transferred to nitrocellulose paper. Three identical blots were stained with antibodies against smooth- and non-muscle myosin II (top row), MHC-A (middle row), or MHC-B (bottom row). The portion containing the myosin heavy chains is shown for each blot; no antibody staining was detected elsewhere on the blots. Gels were loaded to give approximately equal amounts of myosin in each lane. Extracts from BAECs were recognized by all three antibodies, indicating that they contain both A and B heavy chains of myosin II.
(B) Distribution of MHC-A in BAECs. Monolayer cultures of BAEC were 'wounded' by scraping away part of the monolayer with a razor blade. 6 hours later, the cells were fixed and stained by indirect immunofluorescence with an antibody against MHC-A. Cells were migrating in the direction of the large arrow, and dotted lines indicate the leading edge of the cells. MHC-A was distributed predominantly in fibrous structures, many of which displayed periodic striations (e.g. fiber between arrowheads). (C) Distribution of MHC-B in BAECs. Cells were treated as in B, except that they were stained with antibody against MHC-B. Like MHC-A, MHC-B was localized in striated fibers (arrowheads). Note, however, that very little staining occurred in the broad lamellipodia at the cells' leading edges when compared with MHC-A.

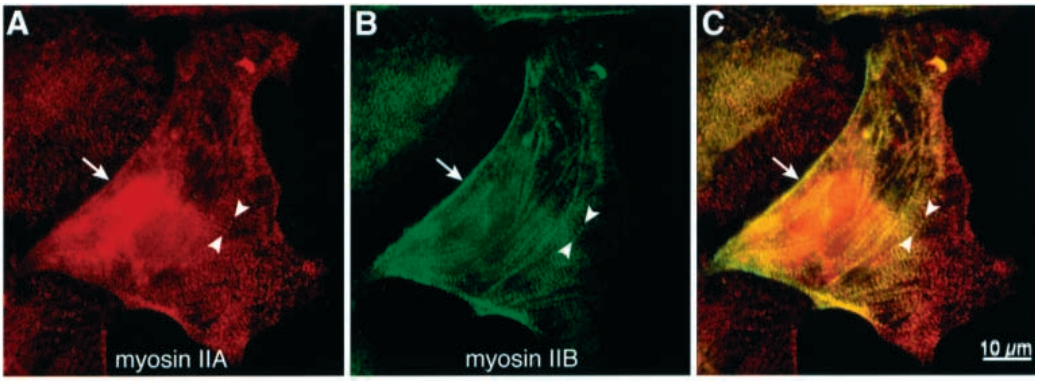


**Fig. 2.** Double immunolocalization of endogenous myosins IIA and IIB in BAECs. Monolayer cultures of BAECs were 'wounded', and fixed 3 hours later. They were then stained by direct immunofluorescence using a cy5-labeled antibody against MHC-A and a rhodamine-labeled antibody against MHC-B. (A) The distribution of MHC-A, (B) the distribution of myosin IIB and (C) an overlay of the two images. The 'wound' is on the right-hand side of the images, so cells were migrating from left to right at the time of fixation. The central cell in the image was extending a large lamellipodium toward the lower right and smaller protrusions along most of its right-hand edge. Note that all these protrusions are clearly visible in the MHC-A image, whereas very little MHC-B staining is present; these regions appear red or orange in the overlay. In contrast, the trailing edges of the cell stain intensely for MHC-B (arrows), but less strongly for MHC-A, so that they appear green in the overlay. Most of the stress fibers in the central and trailing portions of the cell are yellow in the overlay, indicating they contain both MHC-A and MHC-B. The co-localization of MHC-A and MHC-B in the same structure is particularly apparent in the periodic arrays along stress fibers (e.g. the row of four spots between the arrowheads).

It was not obvious that any specific structures contained only MHC-A or MHC-B. However, antibody against MHC-A strongly stained lamellipodia, whereas staining for MHC-B tended to be weak near the periphery of the cell so that lamellipodia were often hard to see.

To further examine this subtle difference between MHC-A and MHC-B, their distributions were examined simultaneously using double-label, direct-staining immunofluorescence (Fig. 2). These observations were made after creating a 'wound' in a confluent culture by scraping away a portion of the endothelial monolayer. This was done so that a large proportion of cells would have well-polarized lamellipodia extending predominantly from one side of the cell. When such cells were stained for MHC-A and MHC-B, the staining patterns could be precisely superimposed on one another over large portions of the cell. However, toward the front of the cell the abundance

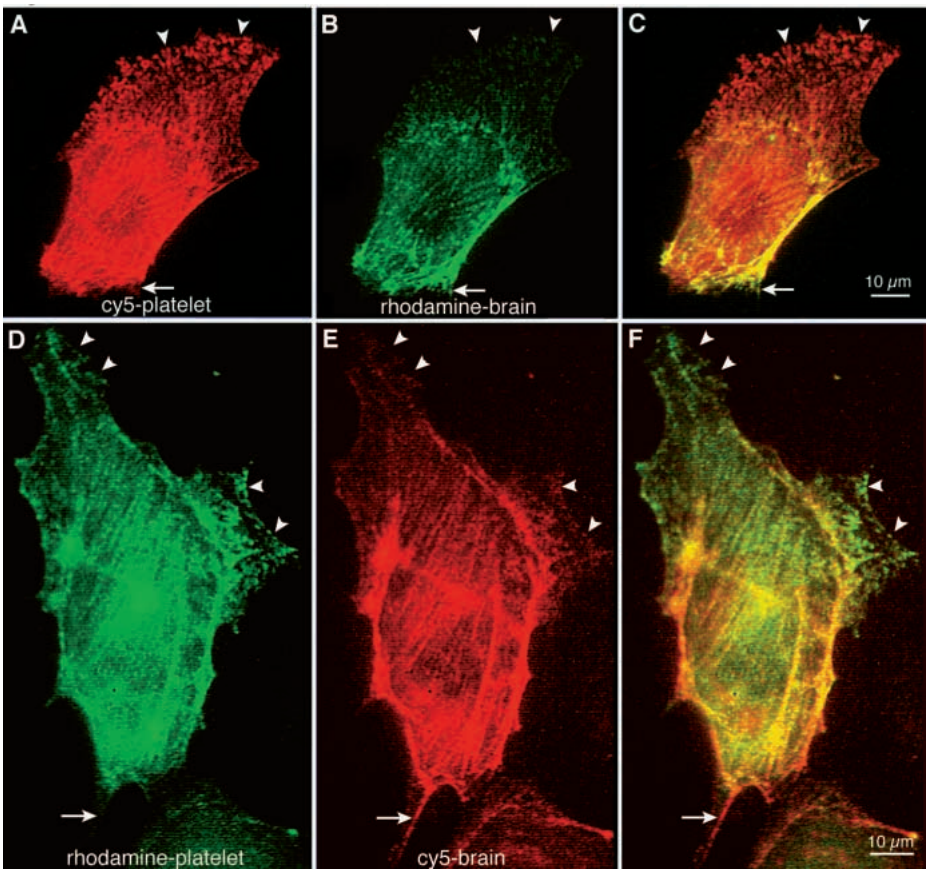


**Fig. 3.** Distribution of microinjected platelet myosin IIA and brain myosin II. Confluent monolayers of BAECs were scrape-wounded, and cells at the edge of the wound were microinjected 1 hour later with a mixture of cy5-labeled platelet myosin IIA and rhodamine-labeled brain myosin II (A-C), or a mixture of rhodamine-labeled platelet myosin IIA and cy5-labeled brain myosin II (D-F). 6 hours after microinjection, separate fluorescence images of the unfixed, living cells were acquired for each of the injected myosins. Cy5 images are illustrated in red (A and E), and rhodamine images in green (B and D). The cy5 and rhodamine images are superimposed in C and F. The cell illustrated in A-C was migrating toward the top of the figure; the cell in D-F was migrating from left to right. Platelet myosin IIA distributed well into the lamellipodia at the cells' leading edges (arrowheads), whereas little brain myosin II was detected at the leading edges, even when structures in other regions of the cell displayed maximal intensity. Conversely, brain myosin II, but not platelet myosin IIA, was visible in some retraction fibers at the trailing edge of the cell (arrows). Note that there is considerable overlap in the distribution of platelet myosin IIA and brain myosin II in the middle of the cells, particularly along stress fibers.

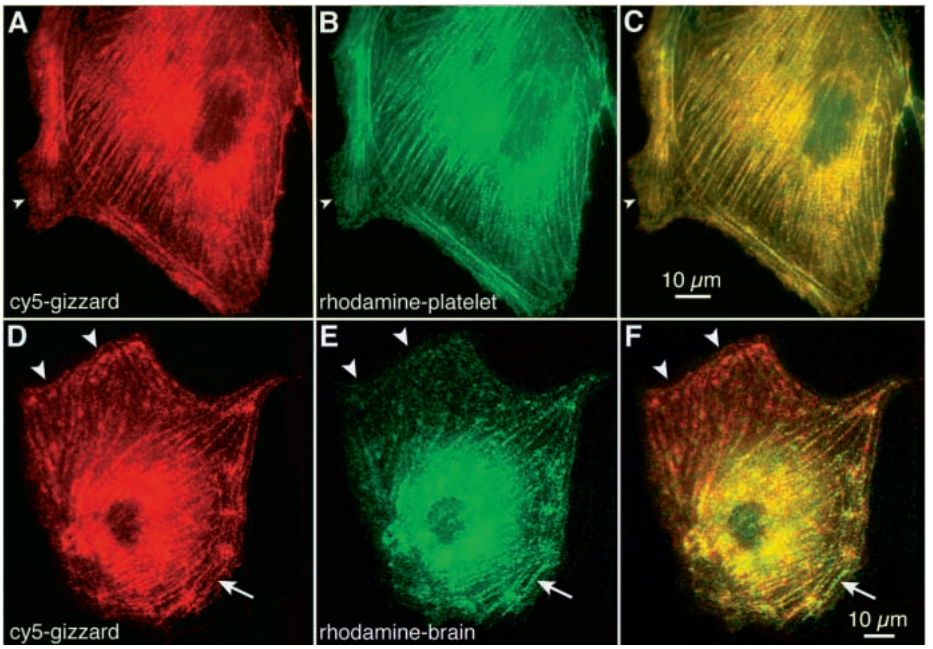


**Fig. 4.** Comparison of microinjected smooth- and non-muscle myosin II. BAECs at the edge of a scrape wound were microinjected with cy5-labeled gizzard (smooth-muscle) myosin II and either rhodamine-labeled platelet myosin IIA (A-C), or rhodamine-labeled brain myosin II (D-F). Images were acquired 6 hours after microinjection. There is very little difference between the distribution of cy5-labeled gizzard myosin II (A) and rhodamine-platelet myosin II (B), which are superimposed in C. Note that there is no preferential distribution of gizzard or platelet myosin II in the lamellipodium at the front of the cell (small arrowheads). In contrast, gizzard myosin II does predominate over brain myosin II in lamellipodia as shown in D-F (large arrowheads). Near the trailing edge, fibers are occasionally observed in which relatively little gizzard myosin II is present while brain myosin II is clearly present (arrows).

of MHC-B declined, while MHC-A persisted very close to the cell's leading edge. This can be seen most clearly when the two staining patterns are overlaid in different colors (Fig. 2C).

At the trailing edge of the cell, unequal staining was also found, but over a much narrower region (Fig. 2, arrows). Along this edge, MHC-B was more abundant. This was not due to misregistration of the images, as specific structures that were visible in both fluorescence channels could be exactly superimposed throughout the image (e.g. Fig. 2, between the arrowheads).

## Distribution of microinjected platelet myosin IIA and brain myosin IIB

Myosins IIA and IIB may possess intrinsic properties that cause them to move to different locations in the cells. Alternatively, they may be synthesized at different sites or turned over at different rates, resulting in different spatial distributions. In order to determine if myosins IIA and IIB are inherently able to sort to different locations in the cell, we examined the behavior of fluorescently labeled, exogenous myosins IIA and IIB when they were microinjected into BAECs.

When cy5-labeled platelet myosin IIA and rhodamine-labeled brain myosin II (predominantly myosin IIB) were co-injected into BAECs, they distributed differently in the cytoplasm. As illustrated in Fig. 3, the differences between injected platelet myosin IIA and brain myosin II closely paralleled the differences observed between endogenous MHC-A and MHC-B. That is, platelet myosin IIA was relatively more abundant near the leading edge of migrating cells than was brain myosin II, while brain myosin II predominated at the extreme trailing edge. In the middle regions of the cell and in large stress fibers, the two myosins were mostly co-distributed.

The same pattern was observed when the dyes were reversed; i.e. when rhodamine-labeled platelet myosin IIA was

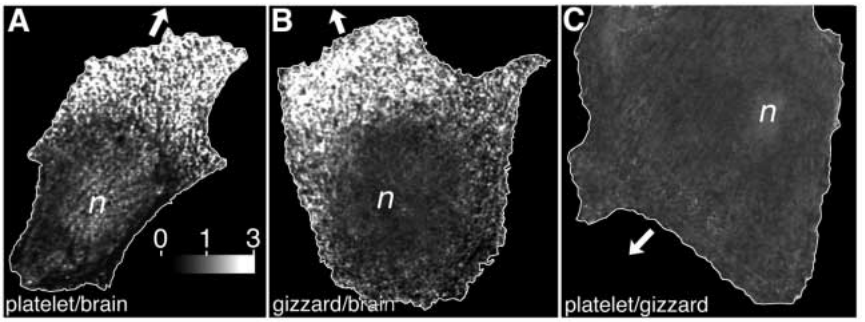


**Fig. 5.** Comparison of myosin distributions by ratio imaging. Ratio images were calculated from paired images of rhodamine- and cy5-labeled myosins as described in Materials and methods. Ratio values are displayed as gray levels that are linearly proportional to the ratio, as indicated by the shaded bar in (A). In order to display most of the cell in visibly distinguishable shades of gray, the maximum on the scale (white) is 3.0. The small number of pixels with ratio values that are greater than 3.0 are also displayed as white. In order to separate low ratios in the periphery of the cell from the black background, the border of the ratio image is outlined by a thin white line that does not represent ratio values. Arrows indicate the direction of movement of each cell. (A) Ratio of cy5-labeled platelet myosin II to rhodamine-labeled brain myosin II. This is the same cell as in Fig. 3A-C. Note the high ratios over the front third of the cell, and the very low ratios along the trailing edge. (B) Ratio of cy5-labeled gizzard myosin II to rhodamine-labeled brain myosin II (same cell as Fig. 4D-F). As in A, ratios are high in the leading third and low in the trailing third of the cell. (C) Ratio of cy5-labeled gizzard myosin II to rhodamine-labeled platelet myosin II (same cell as Fig. 4A-C). This ratio image is very homogeneous. All regions show similar, intermediate grays, indicating equal spatial distribution of platelet and gizzard myosin II. n, location of nucleus.

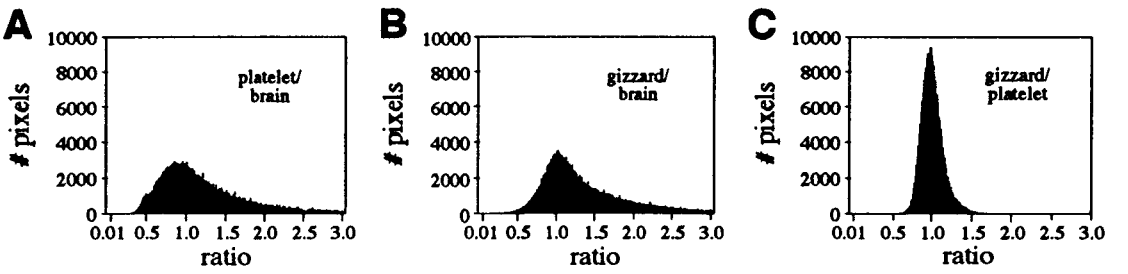


**Fig. 6.** Values of myosin:myosin ratios in microinjected cells. Histograms of the individual pixel values in representative ratio images are shown. (A) Platelet myosin IIA versus brain myosin II, (B) gizzard myosin II versus brain myosin II and (C) gizzard myosin II versus platelet myosin IIA. Images of similar size were chosen so that the total number of pixels in each histogram is approximately the same. All three histograms have their major peak at 1.0, indicating considerable overlap in the distributions of the two myosins. However, note the broad distribution of ratios between platelet and brain myosin II (A) or gizzard and brain myosin II (B), compared to the sharp peak observed when platelet and gizzard myosins are compared (C). Only non-zero ratios (>0.01) are included in order to eliminate regions of the images where no myosin was present. In addition, ratio values >3.0 are not shown so that the bulk of the histogram can be seen clearly; fewer than 5% of the pixels exceeded this range.

co-injected with cy5-labeled brain myosin II (Fig. 3D-F). This indicated that the different distributions were due to properties intrinsic to the myosins, not the attached dyes. It seems most likely that this is due to the predominant isoforms (myosin IIA in platelet and myosin IIB in brain) distributing differently. In addition, the same pattern was observed regardless of which image was acquired first, indicating that the differences were not due to movement of the cells between images.

### Distribution of microinjected smooth-muscle myosin II in endothelial cells

Because fluorescently labeled smooth-muscle myosin II has been used extensively to study myosin dynamics in non-muscle cells, we also compared the distributions of microinjected platelet and brain myosin II with that of smooth-muscle myosin II prepared from turkey gizzards. When fluorescently labeled, turkey-gizzard myosin II was co-injected into BAECs with platelet myosin IIA, the distributions of the two myosins were virtually indistinguishable (Fig. 4A-C). In contrast, the distribution of gizzard myosin II was significantly different from fluorescently labeled brain myosin II (Fig. 4D-F). The proportion of gizzard myosin II relative to brain myosin II was notably higher in lamellipodia, and lower toward the cells' trailing edges.

### Quantitative assessment of local 'sorting' of myosin II isoforms

The distributions of different myosins were compared more quantitatively by creating ratio images (Bright et al., 1987). The fluorescence images of two different myosins that had been co-injected into the same cell were normalized to the same total intensity in order to correct for any differences in the brightness or detection of the fluorophores. Then one image was divided by the other to produce a third image, in which the value at each pixel was equal to the relative proportion of the two myosins at that location in the cell. This provides a direct measure of the degree to which one or the other myosin preferentially localizes at each site in the cell. Typical ratio images (for the cells illustrated in Figs 3, 4) are shown in Fig. 5. Because ratio images indicate relative proportions of two myosins rather than the total amount of myosin at any given location, they are independent of cell thickness. In addition, unlike images in which two myosin distributions are

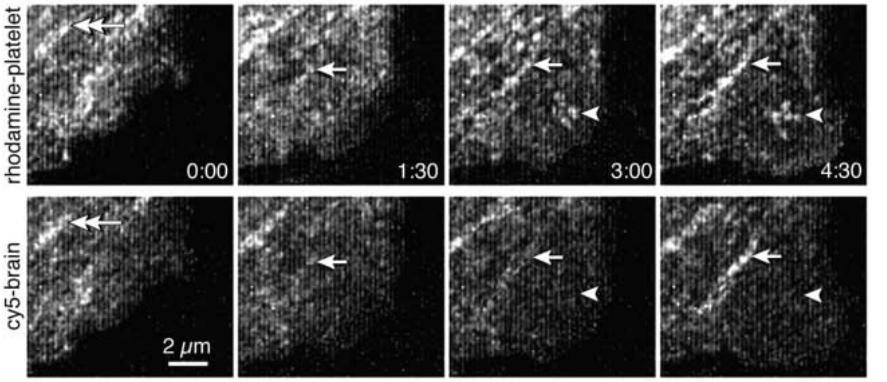


**Fig. 7.** Dynamics of platelet and brain myosin II in an advancing lamellipodium. BAECs migrating at the edge of a scrape wound were microinjected with a mixture of rhodamine-labeled platelet myosin IIA and cy5-labeled brain myosin II. 6 hours after microinjection, pairs of fluorescence images were acquired at 30-second intervals. This figure depicts a small region at the leading edge of a migrating BAEC. The top row of images shows the distribution of platelet myosin IIA, with the time (t) indicated in minutes:seconds at the lower right of each panel. The bottom row of images show the distribution of brain myosin II in the same field at approximately the same time (1-2 seconds elapsed between acquisition of the two images). The double-headed arrow at t=0:00 points to a short, oblong aggregate containing both platelet and brain myosin II with roughly equal intensities. At t=1:30, a fiber began to appear in the platelet myosin IIA sequence, was clearly visible by t=3:00, and continued to grow in size and intensity through t=4:30 (single-headed arrows). Brain myosin II was only faintly apparent in this fiber at t=3:00 and was not clearly evident until t=4:30. Meanwhile, at t=3:00, platelet myosin IIA formed another aggregate (arrowheads) as the leading edge continued to advance toward the lower right. Note that, even at t=4:30, little or no brain myosin II had incorporated into this newest structure.

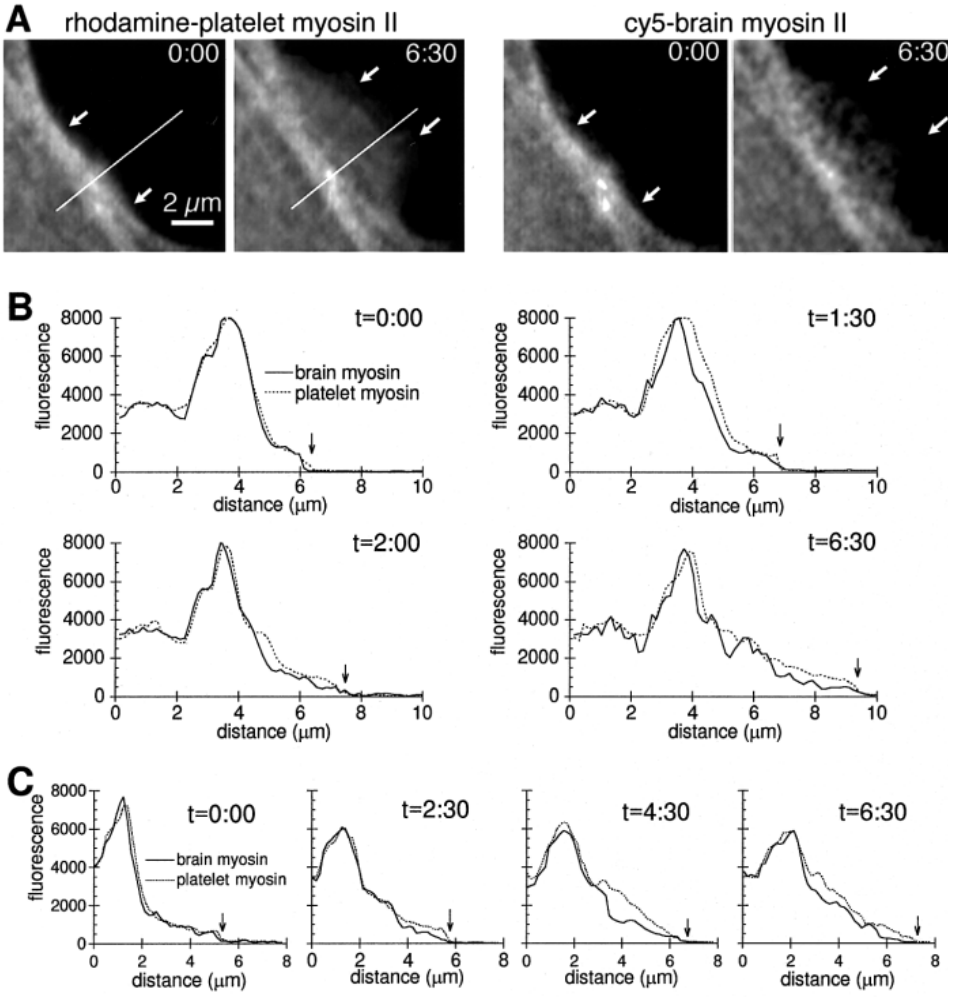


**Fig. 8.** Entry of platelet and brain myosin II into new protrusions. The distribution of platelet and brain myosin II was monitored by time-lapse fluorescence imaging as lamellipodia formed at the edge of a microwound. Background fluorescence was subtracted from each image, then the images were normalized, as described in Materials and methods, so that the total fluorescence intensity of the cell was the same for each image. (A) High-magnification views of the edge of the cell (arrows) where the adjacent cell was removed. Time (t) after wounding (minutes:seconds) is indicated in the upper right of each panel. The white lines in the rhodamine images mark the location of the intensity profiles shown in B. At t=0:00, both rhodamine-platelet and cy5-brain myosin II extend to the edge of the cell. At t=6:30, however, only the platelet myosin II can be seen at the leading edge of the cell (arrows). Brain myosin II is not detected near the edge of the lamellipodium even though its fluorescence in the more peripheral cytoplasm is equal to that of platelet myosin IIA. (B) The fluorescence intensity for each myosin II analog was measured along the line shown in A during extension of the new lamellipodium. Arrows mark the location of the edge of the cell at each timepoint. At the time of wounding, the profiles are almost identical, but at each subsequent timepoint there is consistently more fluorescence from platelet myosin IIA than from brain myosin II in the newly formed regions. (C) A set of intensity profiles was obtained from a different cell with the fluorescence labels reversed; i.e. the cell was microinjected with cy5-platelet myosin II and rhodamine-brain myosin II. Again, the platelet myosin IIA enters the new lamellipodium more rapidly than does the brain myosin II.

superimposed, ratio images do not emphasize structures in which myosin II is concentrated unless those structures contain disproportionate amounts of one myosin.

The extent to which different injected myosins preferentially moved toward the front or rear of migrating cells was assessed as follows. Ratio images comparing platelet or gizzard myosin II with brain myosin II were divided along the cell's axis of migration into leading, trailing and middle zones as described in Materials and methods. The average ratio in each region was then determined. The results are listed in Table 1, and confirmed that platelet myosin IIA distributed more prominently in the front of the cell than did brain myosin II, while brain myosin II was more prominent near the trailing edge. Note that the two myosins were injected as a single, uniform solution. Thus, the different distributions require that, over time, the two isoforms move differently through the living cell. Interestingly, the ratio images did not reveal many specific structures in which only one form of myosin II became concentrated (Fig. 5), suggesting a more global, and less structure-specific, cue for the differences in distribution.

No significant differences were observed in the distributions of platelet and gizzard myosin II among the three regions, and the ratio images were of uniform intensity over the entire cytoplasm. Typical histograms of the actual ratio values from such images are shown in Fig. 6. Within a single cell, ratios of platelet to gizzard were strongly clustered around 1.0. On average, 85.1±4.2% ($n$=6) of the pixels in a platelet:gizzard ratio image have ratios between 0.8 and 1.2. In contrast, the ratio of platelet myosin IIA to brain myosin II varied widely (Figs 5A, 6A); only 40.8±2.7% ($n$=7) of pixels had ratios between 0.8 and 1.2. Similar values (42.3±7.1%, $n$=5) were obtained when gizzard myosin II was compared to brain myosin II.

### Differences in the intracellular dynamics of platelet and brain myosin II

How do platelet myosin IIA and brain myosin II become differentially distributed? This question was examined more closely by following the movements of platelet and brain myosin II as cells moved. As BAECs migrated at the edge of a wound, myosin II-containing structures (e.g. punctate aggregates and stress fibers) continuously formed near the front of the cell in the leading lamellipodia, but some distance (typically 2-5 μm)

**Table 1. Regional variations in the relative distributions of different myosins**

| | Leading edge | Middle | Trailing edge |
|---|---|---|---|
| Ratio of platelet myosin IIA to brain myosin II (mean ± s.e.) | 1.55±0.11 | 1.02±0.05 | 0.70±0.05 |
| Ratio of platelet myosin IIA to gizzard myosin II (mean ± s.e.) | 0.98±0.15 | 1.02±0.11 | 0.96±0.05 |

behind the leading edge. This behavior has been previously reported by several different investigators (DeBiasio et al., 1988; McKenna et al., 1989; Verkhovsky et al., 1995). In our cells, most of these newly forming structures maintained a fixed position relative to the substratum as the cell moved forward. However, occasionally they were observed to move in a retrograde direction (i.e. away from the edge, toward the perinuclear cytoplasm). Such movement typically involved small aggregates that formed close to the cell's leading edge. When aggregates or fibers were examined in central regions of the cell (>5 μm from an edge), they invariably contained both platelet myosin IIA and brain myosin II, and there was no discernible difference in the dynamic behavior of the two myosins. However, close examination of the advancing edge of cells revealed that platelet myosin IIA assembled into fibers and aggregates before brain myosin II did (Fig. 7). This suggests that myosin IIA was moving more rapidly than myosin IIB en route to these structures.

Myosin IIA may appear in specific structures more rapidly than myosin IIB because it coalesces faster within the lamellipodium, or because it enters the lamellipodium more quickly so that its concentration is higher at the location of the incipient structure. To determine if myosin IIA moves into lamellipodia more rapidly than does myosin IIB, isoform dynamics were examined during the initial formation of protrusions. Confluent BAECs were microinjected with fluorescent analogs of brain- and platelet-myosin II, and microwounds were made as described in Materials and methods. The redistribution of myosin II was examined in high-magnification images acquired as lamellipodia formed at the newly exposed free edges of the monolayer. 1-3 lamellipodia were examined on each of 11 different cells, with 8 of the cells containing rhodamine-platelet myosin II and cy5-brain myosin II, and the remaining 3 containing cy5-platelet and rhodamine-brain myosin II. In every case, platelet myosin II appeared in the newly forming protrusion more rapidly than did brain myosin II. This was most apparent at the leading edge of the lamellipodia, where the detectable margin of the platelet analog typically extended beyond that of the brain analog as the edge of the cell advanced (Fig. 8A). Measurements of the fluorescence signal from the analogs allowed tracking of the bulk entry of each myosin into the lamellipodium, independent of the visibility of specific structures such as fibers or the edge of the cell (Fig. 8B,C). Direct comparison of the two signals in the lamellipodia confirmed that platelet myosin II accumulated in the new protrusion more rapidly and more distally than did brain myosin II. This was not due to movement of the edge between acquisition of the two images, because very little movement occurred during the 1-2 seconds that elapsed between images, and platelet myosin II preceded brain myosin

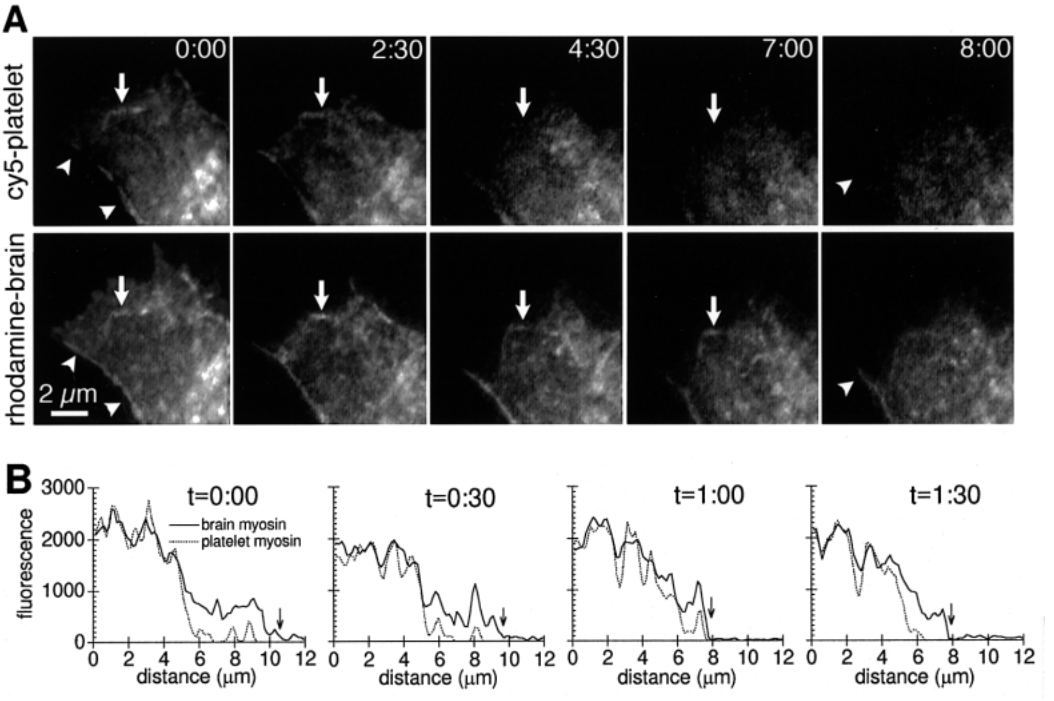


**Fig. 9.** Dynamics of platelet and brain myosin II in retracting cytoplasm. BAECs were microinjected with a mixture of cy5-labeled platelet myosin IIA and rhodamine-labeled brain myosin II. 4 hours after microinjection pairs of fluorescence images were acquired at 30-second intervals as the cell migrated toward the lower right of the field. The micrographs in (A) depict a small region at the trailing edge as it retracts. The top row of images shows the distribution of platelet myosin II, with the time (t) indicated in minutes:seconds at the upper right of each panel. The bottom row of images show the distribution of brain myosin II in the same field 1-2 seconds later. As the cell moved, both platelet and brain myosin II disappeared from this region. However, brain myosin II persisted in many areas well after platelet myosin II was no longer detectable. For example, at t=4:30, platelet myosin II begins to disappear from a small linear structure in the peripheral cytoplasm (arrows) and is virtually completely absent by t=7:00, while brain myosin is still clearly visible. Also compare the retention of platelet and brain myosin II in the stress fiber at the lower left (arrowheads at t=0:00 and 8:00). (B) Intensity profiles from the trailing region of a migrating cell. Arrows mark the location of the trailing edge of the cell. Although fluorescence intensities for platelet and brain myosin II are equivalent in the more proximal part of the profile, in the distal regions of the retracting cytoplasm, brain myosin II is consistently more abundant than the platelet analog.

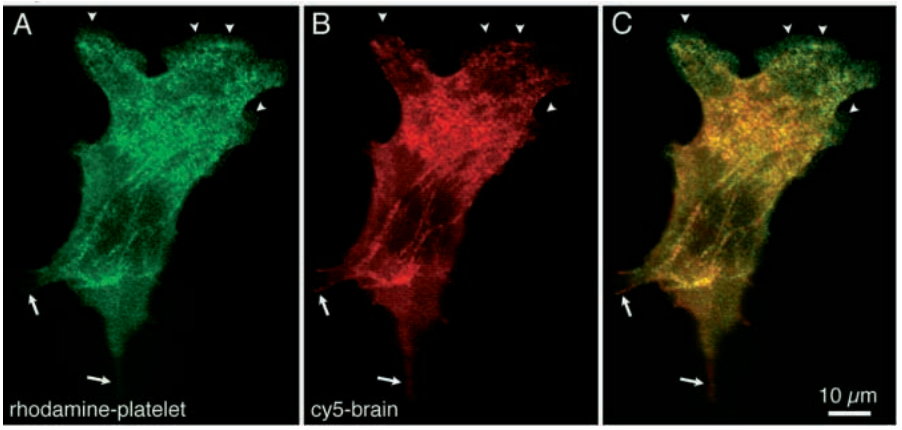


**Fig. 10.** Microinjected platelet and brain myosin II in COS fibroblasts. Confluent monolayers of COS fibroblasts were wounded and cells at the edge of the wound were microinjected 1 hour later with a mixture of rhodamine-labeled platelet myosin IIA and cy5-labeled brain myosin II. 4 hours after microinjection, separate fluorescence images of the unfixed, living cells were acquired for each of the injected myosins. The direction of migration is toward the top of the image. Both platelet myosin IIA (A) and brain myosin II (B) incorporated into stress fibers and small aggregates and distributed diffusely in the perinuclear cytoplasm. There was little or no difference in the distribution of the two myosins in the central regions of the cell, as indicated by the yellow color over most of the cell when the green and red images are superimposed (C). In the periphery of the cell, platelet myosin II was more abundant than brain myosin II in the lamellipodia at the leading edge (arrowheads), which appear green in the overlay. Conversely, brain myosin II predominated in the cell's retracting tails (arrows), and these appear orange or red in the overlay.

II regardless of which image was acquired first. Nor could the difference be attributed to platelet myosin II being detected more easily than brain myosin II, because (1) approximately equal concentrations of the two analogs were injected, (2) images were normalized so that the total fluorescence signal from each analog was the same and (3) the difference was observed regardless of which myosin II was labeled with which dye. Furthermore, the measured intensities of the platelet and brain analogs differed in the advancing protrusion, even when their intensities in the 'older', more proximal cytoplasm were equivalent prior to formation of the protrusion.

The converse phenomenon was observed in retracting cytoplasm at the trailing edge of migrating cells. Although disassembly of myosin-containing structures was less gradual than the assembly at the leading edge (usually occurring concomitant with detachment and rapid retraction of the edge), brain myosin II was nonetheless occasionally observed to persist in fibers at the trailing edge of the cell after platelet myosin IIA had dissipated (see Fig. 4). High magnification, time-lapse imaging of the rear edge of migrating cells showed that brain myosin II was retained in retracting structures for longer periods than equivalent amounts of platelet myosin II (Fig. 9). Thus, while both forms of myosin II became incorporated into the same structures, they redistributed at different rates: platelet myosin IIA incorporated and released more rapidly than brain myosin II.

### 'Sorting' is independent of endogenous myosin IIA

Microinjected platelet and brain myosin II do not sort simply by associating with endogenous myosin. This was demonstrated by microinjecting analogs into COS fibroblasts, which contain myosin IIB, but not myosin IIA (see Fig. 1). As illustrated in Fig. 10, the distribution of platelet and brain myosin II in COS cells was similar to the distribution in BAECs. That is, the two analogs colocalized through most of the cytoplasm, but platelet myosin II predominated at the leading edge and brain myosin II predominated in retracting regions of the tail.

## DISCUSSION

### Myosin II isoforms can specify their own distribution

When exogenous myosin II is added to the cytoplasm of living endothelial cells, it moves (or is moved) into a distribution that is dependent on the isoform. Exogenously added platelet myosin II, which essentially contains only the A isoform of the myosin heavy chains, assumes a distribution that is analogous to that of endogenous myosin IIA, while the distribution of exogenously added brain myosin II, which is predominantly the B isoform, parallels that of endogenous myosin IIB. The differences between exogenously added myosins is important because it demonstrates that different isoforms can 'find' their correct distributions in the cell. This indicates that different localizations are due to properties inherent to the protein, and not simply a function of localized synthesis or turnover. In other words, the cytoplasm possesses spatial cues that are recognized in slightly different ways by different myosin II isoforms.

When isoform distribution is determined by immunofluorescence, apparent differences could actually be due to local masking of an isoform-specific epitope. This is particularly likely to occur when the differences between isoforms are small, as with MHC-A and MHC-B, or if the molecule in question undergoes extensive assembly or binding with other molecules, as does myosin II. Since the fluorescence of an injected analog does not require that the molecule be accessible to an antibody, and because fluorophores are attached at multiple sites, isoform-specific analogs cannot be masked. Thus, the different localization of isoform-specific fluorescent analogs represents a definitive demonstration of isoform-specific distribution.

Although brain and platelet myosin II distribute differently, it does not appear that there are any discrete structures in BAECs that contain only one particular isoform. This is emphasized by ratio images, which show very little structure, but instead reveal graded differences in distribution across the cell. This suggests that myosin IIA and B are not homing to different cytoplasmic 'receptors' and are not assembling into, or binding onto, different local structures. Rather, they appear to be responding to broader, more global cues. For example, locomoting amoeba (Taylor et al., 1980), eosinophils (Brundage et al., 1991) and fibroblasts (Hahn et al., 1992) all display gradients in intracellular free $Ca^{2+}$. If the distributions of myosin IIA and B are polarized by this gradient, but the two isoforms do not respond equally, this could lead to the different distributions.

### Distinct isoform distributions reflect different dynamic equilibria

One obvious way in which the responses of myosins IIA and IIB could differ is in their speed. In vitro, myosin IIA moves actin filaments three times faster than myosin IIB does, and also displays a higher actin-activated ATPase activity (Kelley et al., 1996). Fluorescent analogs permit examination of the dynamic behavior of myosin II isoforms within living cells, to determine if such in vitro differences may be recapitulated in the cytoplasm, and the dynamics of movement of microinjected brain and platelet myosin II reported in the present paper suggest that they are. That is, myosin IIA appears to move more rapidly through the cell than does myosin IIB: it enters newly forming structures faster, and is also first to leave disassembling structures. Since the cytoskeleton is continually being remodeled, any given snapshot of the cell reveals a relative abundance of myosin IIA in nascent structures and a preponderance of myosin IIB in dissipating structures, with long-lived structures like stress fibers accumulating both forms. However, our observations do not indicate whether or not this difference is due directly to a faster motor activity of myosin IIA. On the one hand, platelet myosin II could move into new protrusions more rapidly than brain myosin II because myosin IIA travels faster than myosin IIB along actin-filament tracks into the protrusion. We have previously shown that relatively little of the myosin II in the leading edge of migrating cells is freely diffusing even when it is not assembled into discrete fibers (Kolega and Taylor, 1993; Kolega, 1997). On the other hand, myosin IIA could also enter new protrusions more rapidly if it dissociates from existing structures more quickly (perhaps due to more rapid turnover of ATP) and so becomes available sooner than myosin IIB. More precise measurements of the local molecular mobilities and velocities will be required to distinguish between these possibilities.

### Myosins IIA and IIB isoforms in other cells

The relative distribution of MHC-A and MHC-B in BAECs is very similar to that observed in human melanoma and HeLa cells during interphase (Maupin et al., 1994). The distribution in nerve cells is somewhat different, but is still consistent with a more rapid redistribution of myosin IIA. For example, there is a prevalence of myosin IIB in retracting portions of nerve growth cones (Rochlin et al., 1995), and myosin IIA tends to be more uniformly distributed in the peripheral growth cone (see Rochlin et al., 1995, Fig. 2). In addition, because there is a continuous retrograde flow of cytoskeleton in the growth cone, differences in the rates of redistribution for myosins IIA and IIB would also account for the observed enrichment of MHC-B at the base of the growth cone's broad peripheral cytoplasm (the 'marginal zone' of Rochlin et al.) since this region contains the longest-lived cytoskeletal structures.

There is one published report in which the distributions of MHC-A and MHC-B are strikingly different from those discussed above. In Xenopus A6 cells, there is very little overlap in the distribution of MHC-A and MHC-B (Kelley et al., 1996). Curiously, in A6 cells it appears that MHC-B is found predominantly in lamellipodia, which presumably contain a very dynamic cytoskeleton, while MHC-A tends to localize in stress fibers and distribute diffusely in the perinuclear cytoplasm. The reason for this apparent reversal of distributions is unclear. However, it should be noted that, in the A6 study, MHC-A and MHC-B were never localized in the same cell by double-staining. Rather, each isoform was compared separately to a third cytoskeletal element, i.e. microfilaments or microtubules. In addition, the locomotive behavior of stained cells was only inferred from morphology, and not determined directly by time-lapse imaging as was done for BAECs and for nerve growth cones.

### Smooth muscle myosin II behaves as non-muscle myosin IIA

Surprisingly, the behavior of smooth-muscle myosin II was indistinguishable from that of non-muscle myosin IIA when both were injected into endothelial cells. Although it remains to be seen whether these isoforms co-localize during the cytoskeletal reorganizations associated with mitosis and cytokinesis, it is striking that their behavior is equivalent through all the complex cytoskeletal rearrangements of endothelial locomotion; i.e. lamellipodial protrusion, retrograde movement of fibers and aggregates, stress fiber contraction and disassembly, and tail retraction. This observation is reassuring in light of the many studies of non-muscle cells that have used fluorescent analogs of smooth-muscle myosin II to infer the dynamics of endogenous myosin II (DeBiasio et al., 1988; Giuliano et al., 1992; Giuliano and Taylor, 1990; Kolega, 1997; Kolega et al., 1991, 1993; Kolega and Taylor, 1993; McKenna et al., 1989; Sanger et al., 1989; Verkhovsky et al., 1995). The present study provides validation, at least for endothelial cells, that smooth-muscle analogs provide a good indicator of the behavior of the A isoform of non-muscle myosin II. However, it also leaves open the question of how the B isoform behaves. Given the aforementioned differences in the distribution of MHC-A and MHC-B in a variety of different systems, this is an important issue to resolve.

### The role of different myosin II isoforms in nonmuscle motility

Why do multiple isoforms of myosin II exist in non-muscle cells? On the one hand, the extensive overlap in the distributions of myosins IIA and B in endothelial, HeLa and human melanoma cells suggest that they do not perform distinct functions. Furthermore, many cells, such as platelets, COS fibroblasts and a variety of avian cells (Conrad et al., 1995), appear to function normally with only one isoform, suggesting that the isoforms can readily substitute for one another. These observations prompt the hypothesis that different isoforms merely reflect the existence of different, but functionally equivalent, myosin II genes, and that different isoforms are expressed purely on the basis of which gene cassettes are turned on for that particular cell type (Maupin et al., 1994).

On the other hand, the myosins IIA and IIB do have different enzymatic activities, and the present study shows that this is accompanied by different dynamic behaviors in living cells. Moreover, in a number of instances, myosins IIA and IIB segregate dramatically, such as in A6 cells, and during mitosis of a wide variety of different cells (Maupin et al., 1994; Conrad et al., 1995; Kelley et al., 1996). This suggests that sometimes one isoform does perform a specific function better than the other, or that it at least possesses unique regulatory features that cause it to respond with greater temporal/spatial specificity. Given that myosin IIA and IIB motors run at different speeds in vitro, and now appear to move at different rates in cytoplasm

as well, might isoform diversity be a mechanism for controlling the overall speed of myosin II-based movements? The movement of actin filaments by myosin II in in-vitro motility assays is very sensitive to the presence of different isoforms; only small amounts of a slower isoform can dramatically reduce the velocity produced by mixtures of myosin II (Cuda et al., 1997). Thus, variations in the proportions of myosins IIA and IIB could produce a different baseline velocity for a particular cell type or for a particular state of cell activity. This possibility could be tested by a careful examination of myosin II-based movements in cells expressing different amounts of A and B isoforms, such as those that appear spontaneously in cultures of human melanoma cells (Maupin et al., 1994).

This work was supported by a grant from the National Science Foundation (MCB-9417115).

## REFERENCES

**Bright, G. R., Rogowska, J., Fisher, G. W. and Taylor, D. L.** (1987). Fluorescence ratio imaging microscopy: temporal and spatial measurements in single living cells. *Biotechniques* **5**, 556-563.

**Brundage, R. A., Fogarty, K. E., Tuft, R. A. and Fay, F. S.** (1991). Calcium gradients underlying polarization and chemotaxis of eosinophils. *Science* **254**, 703-7706.

**Cheng, T. P. O., Murakami, N. and Elzinga, M.** (1992). Localization of myosin IIB at the leading edge of growth cones from rat dorsal ganglionic cells. *FEBS Lett.* **311**, 91-94.

**Condeelis, J. S. and Taylor, D. L.** (1977). The contractile basis of amoeboid movement. V. The control of gelation, solation and contraction in extracts from *Dictyostelium discoideum*. *J. Cell Biol.* **74**, 901-927.

**Conrad, P. A., Giuliano, K. A., Fisher, G., Collins, K., Matsudaira, P. T. and Taylor, D. L.** (1993). Relative distribution of actin, myosin I and myosin II during the wound healing response of fibroblasts. *J. Cell Biol.* **120**, 1381-1391.

**Conrad, A. H., Jaffredo, T. and Conrad, G. W.** (1995). Differential localization of cytoplasmic myosin II isoforms A and B in avian interphase and dividing embryonic and immortalized cardiomyocytes and other cell types in vitro. *Cell Motil. Cytoskel.* **31**, 93-112.

**Cuda, G., Pate, E., Cooke, R. and Sellers, J. R.** (1997). In vitro actin filament sliding velocities produced by mixtures of different types of myosin. *Biophys. J.* **72**, 1767-1779.

**Daniel, J. L. and Sellers, J. R.** (1992). Purification and characterization of platelet myosin. *Meth. Enzymol.* **215**, 78-88.

**DeBiasio, R. L., Wang, L.-L., Fisher, G. W. and Taylor, D. L.** (1988). The dynamic distribution of fluorescent analogues of actin and myosin in protrusions at the leading edge of migrating Swiss 3T3 fibroblasts. *J. Cell Biol.* **107**, 2631-2645.

**DeLozanne, A. and Spudich, J. A.** (1987). Disruption of the Dictyostelium myosin heavy chain gene by homologous recombination. *Science* **236**, 1086-1091.

**Giuliano, K. A., Kolega, J., DeBiasio, R. L. and Taylor, D. L.** (1992). Myosin II phosphorylation and the dynamics of stress fibers in serum-deprived and stimulated fibroblasts. *Mol. Biol. Cell* **3**, 1037-1048.

**Giuliano, K. A. and Taylor, D. L.** (1990). Formation, transport, contraction, and disassembly of stress fibers in fibroblasts. *Cell Motil. Cytoskel.* **16**, 14-21.

**Hahn, K., DeBiasio, R. and Taylor, D. L.** (1992). Patterns of elevated free calcium and calmodulin activation in living cells. *Nature* **359**, 736-738.

**Hahn, K. M., Kolega, J., Montibeller, J., DeBiasio, R., Post, P., Myers, J. and Taylor, D. L.** (1993). Fluorescent analogs: optical biosensors of the chemical and molecular dynamics of macromolecules in living cells. In *Fluorescent and Luminescent Probes for Biological Activity: A Practical Guide to Technology for Quantitative Real-Time Analysis* (ed. W. T. Mason), pp. 349-359. Academic Press, New York.

**Hoock, T. C., Newcomb, P. M. and Herman, I. M.** (1991). β-Actin and its mRNA are localized at the plasma membrane and the regions of moving cytoplasm during cellular response to injury. *J. Cell Biol.* **112**, 653-664.

**Huxley, H. E.** (1969). The mechanism of muscular contraction. *Science* **164**, 1356-1366.

**Katsuragawa, Y., Yanagisawa, M., Inoue, A. and Masaki, T.** (1989). Two distinct nonmuscle myosin-heavy-chain mRNAs are differently expressed in various chicken tissues. *Eur. J. Biochem.* **184**, 611-616.

**Kelley, C. A., Sellers, J. R., Gard, D. L., Bui, D., Adelstein, R. S. and Baines, I. C.** (1996). Xenopus nonmuscle myosin heavy chain isoforms have different subcellular localizations and enzymatic activities. *J. Cell Biol.* **134**, 675-687.

**Knecht, D. A. and Loomis, W. F.** (1987). Antisense RNA inactivation of myosin heavy chain gene expression in Dictyostelium discoideum. *Science* **236**, 1081-1086.

**Kolega, J.** (1998). Fluorescent analogues of myosin II for tracking the behavior of different myosin isoforms in living cells. *J. Cell. Biochem.* **68**, 1-13.

**Kolega, J.** (1997). Asymmetry in the distribution of free versus cytoskeletal myosin II in locomoting microcapillary endothelial cells. *Exp. Cell Res.* **231**, 66-82.

**Kolega, J., Janson, L. W. and Taylor, D. L.** (1991). The role of solation-contraction coupling in regulating stress fiber dynamics in nonmuscle cells. *J. Cell Biol.* **114**, 993-1003.

**Kolega, J., Nederlof, M. A. and Taylor, D. L.** (1993). Quantitation of cytoskeletal fibers in fluorescence images: stress fiber disassembly accompanies dephosphorylation of the regulatory light chains of myosin II. *Bioimaging* **1**, 136-150.

**Kolega, J. and Taylor, D. L.** (1993). Gradients in the concentration and assembly of myosin II in living fibroblasts during locomotion and fiber transport. *Mol. Biol. Cell* **4**, 819-836.

**Li, D., Miller, M. and Chantler, P. D.** (1994). Association of a cellular myosin II with anionic phospholipids and the neuronal plasma membrane. *Proc. Nat. Acad. Sci. USA* **91**, 853-857.

**Maupin, P., Phillips, C. L., Adelstein, R. S. and Pollard, T. D.** (1994). Differential localization of myosin-II isoforms in human cultured cells and blood cells. *J. Cell Sci.* **107**, 3077-3090.

**McKenna, N. M., Wang, Y.-l. and Konkel, M. E.** (1989). Formation and movement of myosin-containing structures in living fibroblasts. *J. Cell Biol.* **109**, 1163-1172.

**Murakami, N., Mehta, P. and Elzinga, M.** (1991). Studies on the distribution of cellular myosin with antibodies to isoform-specific synthetic peptides. *FEBS Lett.* **278**, 23-25.

**Pasternak, C., Spudich, J. A. and Elson, E. L.** (1989). Capping of surface receptors and concomitant cortical tension are generated by conventional myosin. *Nature* **341**, 549-551.

**Phillips, C. L., Yamakawa, K. and Adelstein, R. S.** (1995). Cloning of the cDNA encoding human nonmuscle myosin heavy chain B and analysis of human tissues with isoform-specific antibodies. *J. Muscle Res. Cell Motil.* **16**, 379-389.

**Rochlin, M. W., Itoh, K., Adelstein, R. S. and Bridgman, P. C.** (1995). Localization of myosin II A and B isoforms in cultured neurons. *J. Cell Sci.* **108**, 3661-3670.

**Sanger, J. M., Mittal, B., Dome, J. S. and Sanger, J. W.** (1989). Analysis of cell division using fluorescently labeled actin and myosin in living PtK2 cells. *Cell Motil. Cytoskel.* **14**, 201-219.

**Sellers, J. R.** (1991). Regulation of cytoplasmic and smooth muscle myosin. *Curr. Opin. Cell Biol.* **3**, 98-104.

**Tan, J. L., Ravid, S. and Spudich, J. A.** (1992). Control of nonmuscle myosins by phosphorylation. *Annu. Rev. Biochem.* **61**, 721-759.

**Taylor, D. L., Blinks, J. R. and Reynolds, G.** (1980). Contractile basis of ameboid movement VIII. Aequorin luminescence during ameboid movement, endocytosis and capping. *J. Cell Biol.* **86**, 599-607.

**Trybus, K. M.** (1991). Assembly of cytoplasmic and smooth muscle myosins. *Curr. Opin. Cell Biol.* **3**, 105-111.

**Verkhovsky, A. B., Svitkina, T. M. and Borisy, G. G.** (1995). Myosin II filament assemblies in the active lamella of fibroblasts: their morphogenesis and role in the formation of actin filament bundles. *J. Cell Biol.* **131**, 989-1002.

**Wessels, D., Soll, D. R., Knecht, D., Loomis, W. F., DeLozanne, A. and Spudich, J.** (1988). Cell motility and chemotaxis in *Dictyostelium* amebae lacking myosin heavy chain. *Dev. Biol.* **128**, 164-177.

**Wessels, D. and Soll, D. R.** (1990). Myosin II heavy chain null mutant of Dictyostelium exhibits defective intracellular particle movement. *J. Cell Biol.* **111**, 1137-1148.

**Wiseman, J. W., Glover, L. A. and Hesketh, J. E.** (1997). Evidence for a localization signal in the 3′ untranslated region of myosin heavy chain messenger RNA. *Cell. Biol. Int.* **21**, 243-248.